gp130 signaling in proopiomelanocortin neurons mediates the acute anorectic response to centrally applied ciliary neurotrophic factor

Ruth Janoschek*, Leona Plum*†, Linda Koch*, Heike Münzberg‡, Sabrina Diano§¶, Marya Shanabrough§, Werner Müller‖, Tamas L. Horvath§¶**, and Jens C. Brüning*††

*Institute for Genetics and Center for Molecular Medicine Cologne, Department of Mouse Genetics and Metabolism, University of Cologne, D-50674 Cologne, Germany; †Klinik II und Poliklinik für Innere Medizin, University of Cologne, D-50931 Cologne, Germany; ‡Division of Metabolism, Endocrinology, and Diabetes, Departments of Internal Medicine and Molecular Physiology, University of Michigan Medical School, Ann Arbor, MI 48109-0638; ‖German Research Centre for Biotechnology, D-38124 Braunschweig, Germany; and Departments of §Obstetrics, Gynecology, and Reproductive Sciences and ¶Neurobiology and **Section of Comparative Medicine, Yale University School of Medicine, New Haven, CT 06519

Edited by Jeremy Nathans, Johns Hopkins University School of Medicine, Baltimore, MD, and approved May 31, 2006 (received for review January 17, 2006)

Ciliary neurotrophic factor (CNTF) exerts anorectic effects by overcoming leptin resistance via activation of hypothalamic neurons. However, the exact site of CNTF action in the hypothalamus has not yet been identified. Using Cre-loxP-mediated recombination *in vivo*, we have selectively ablated the common cytokine signaling chain gp130, which is required for functional CNTF signaling, in proopiomelanocortin (POMC)-expressing neurons. POMC-specific gp130 knockout mice exhibit unaltered numbers of POMC cells and normal energy homeostasis under standard and high fat diet. Endotoxin (LPS) and stress-induced anorexia and adrenocorticotropin regulation were unaffected in these animals. Strikingly, the anorectic effect of centrally administered CNTF was abolished in POMC-specific gp130 knockout mice. Correspondingly, in these animals, CNTF failed to activate STAT3 phosphorylation in POMC neurons and to induce c-Fos expression in the paraventricular nucleus. These data reveal POMC neurons as a critical site of CNTF action in mediating its anorectic effect.

CNS | obesity

Obesity is commonly linked to leptin resistance (1). Physiologically, leptin activates the JAK/STAT signaling pathway through the long form of leptin receptors (ObRb), which belong to the family of cytokine receptors (2). Multiple mechanisms for the development of leptin resistance have been proposed such as reduced transport of leptin across the blood–brain barrier (3), as well as desensitization of the leptin target cells by increased expression of the suppressor of cytokine signaling (SOCS) (4) proteins. One therapeutic approach to overcoming leptin resistance could be to mimic intracellular leptin-evoked signaling through alternative receptors.

The ciliary neurotrophic factor receptor (CNTFR) also belongs to the family of cytokine receptors. In contrast to leptin, CNTF only fully activates this pathway as part of a tripartite complex consisting of CNTFR-α, leukemia inhibitory factor receptor (LIFR) β, and gp130. JAK2 associated with gp130 becomes activated upon homo- or heterodimerization of gp130 resulting in the activation of the JAK/STAT pathway. Both CNTFR-α and gp130 are expressed in neurons of the arcuate nucleus (ARC) of the hypothalamus (5), and CNTF application is able to inhibit food intake and to reduce body weight both in control and leptin-resistant mice (6–9). Pharmacological experiments have indicated that CNTF, similar to leptin, is capable of suppressing neuropeptide Y mRNA levels, and neuropeptide Y application counteracts the weight-reducing effects of CNTF (9). Nevertheless, co-administration of an anorexigenic and an orexigenic factor does not prove that both are part of or targeting the same pathway(s). On the other hand, CNTF and leptin initiate differential patterns of gene expression in the ARC, indicating diverging mechanisms of action and potentially differential target sites of both hormones (10, 11). Currently, it is not known which neuronal subpopulation mediates the effects of CNTF. Because proopiomelanocortin (POMC) neurons are an important primary site of leptin action in the brain and critical for energy homeostasis (12), we have explored the role of these cells in mediating CNTF's biological effect on feeding.

Results

POMC-Restricted Inactivation of gp130. Mice carrying the loxP-flanked (flox) gp130 allele (13) were crossed with mice expressing the Cre recombinase under control of the *Pomc* promoter (14). Cre-mediated recombination was visualized through the use of a reporter mouse strain (*Z/EG*) in which transcription of a green fluorescent protein (GFP) gene under control of the ubiquitously expressed *Rosa26* promoter is prevented by a floxed neomycin-resistance gene (15). These mice showed a pattern of GFP immunoreactivity in the ARC of the hypothalamus similar to POMC (Fig. 1*a*). Consistent with this, Western blot analysis revealed no alterations in overall brain and hypothalamic gp130 protein expression (Fig. 1*b*). Accordingly, gp130 expression in peripheral tissues remained unchanged in $gp130^{\Delta POMC}$ mice (Fig. 1*b*).

Abolished CNTF-Stimulated STAT3 Tyrosine Phosphorylation in POMC Cells of $gp130^{\Delta POMC}$ Mice. To determine the effect of POMC cell-restricted deficiency of gp130 on CNTF's induction of STAT3 phosphorylation, control and $gp130^{\Delta POMC}$ mice expressing β-gal in POMC neurons were injected with recombinant CNTF i.v. In control mice, CNTF treatment resulted in profound activation of STAT3 phosphorylation in both POMC- and non-POMC-expressing neurons of the ARC (Fig. 1*c*). In contrast, in $gp130^{\Delta POMC}$ mice, CNTF stimulation resulted in tyrosine phosphorylation of STAT3 in non-POMC cells, but it failed to activate STAT3 phosphorylation in POMC neurons (Fig. 1 *c* and *d*). To determine the specificity of gp130 ablation in POMC neurons for gp130-dependent cytokine signaling, both control and $gp130^{\Delta POMC}$ mice were treated by i.v. injection of leptin. Leptin treatment evoked a clear stimulation of STAT3 tyrosine phosphorylation in both POMC and non-POMC cells of control and $gp130^{\Delta POMC}$ mice (Fig. 1*c*). These data indicate, that POMC-restricted inactivation of gp130 selectively inhibits the signaling via gp130-coupled cytokine

Conflict of interest statement: No conflicts declared.

This paper was submitted directly (Track II) to the PNAS office.

Abbreviations: CNTF, ciliary neurotrophic factor; i.c.v., intracerebroventricular(ly); POMC, proopiomelanocortin; PVN, paraventricular nucleus.

††To whom correspondence should be addressed at: Institute for Genetics, Department of Mouse Genetics and Metabolism, University of Cologne, Zülpicher Strasse 47, D-50674 Cologne, Germany. E-mail: jens.bruening@uni-koeln.de.

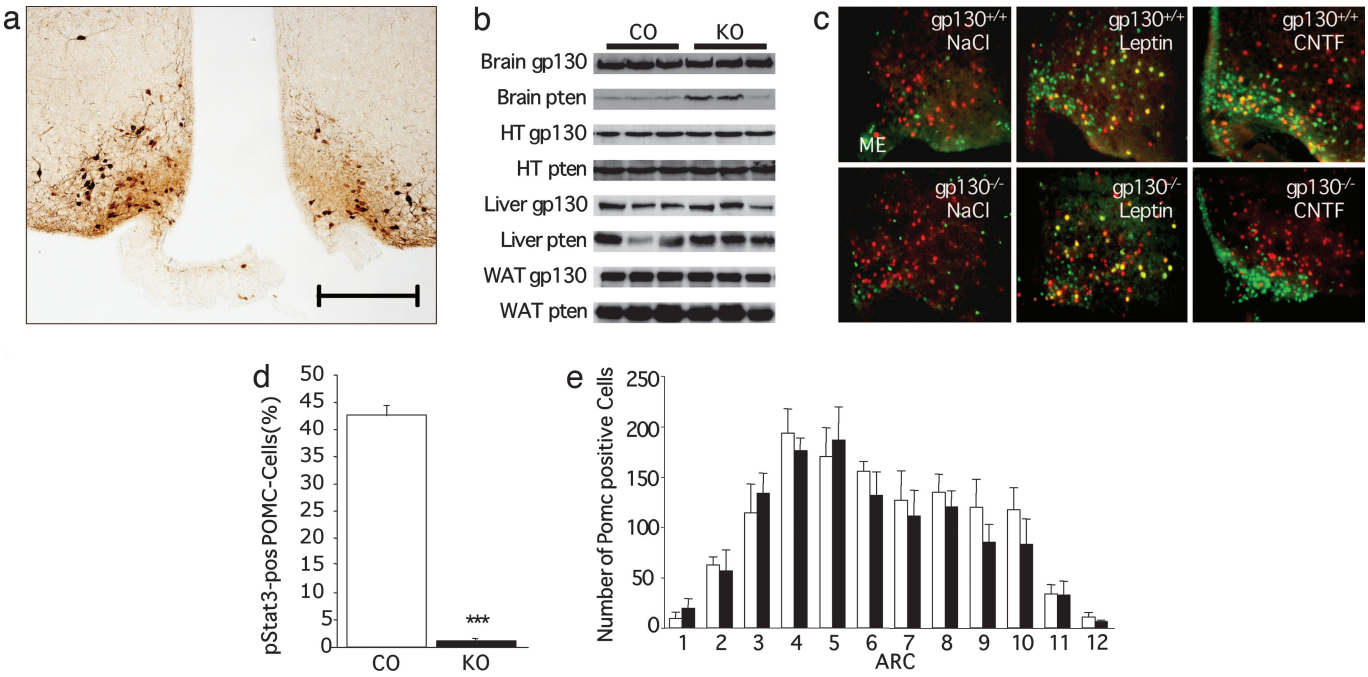

Fig. 1. Generation of POMC-specific knockout ($gp130^{\Delta POMC}$) mice. (*a*) *PomcCre* mice were mated with *Z/EG* reporter mice, and immunohistochemistry for enhanced GFP was performed in double-transgenic mice. (Scale bar: 100 μm.) (*b*) Western blot analysis of gp130 and pten (loading control) in brain, hypothalamus (HT), liver, and white adipose tissue (WAT) in control (CO) and $gp130^{\Delta POMC}$ (KO) mice. (*c*) Double immunohistochemistry for p-STAT3 (green) and β-gal (red) in POMC neurons of control ($gp130^{+/+}$) and $gp130^{\Delta POMC}$ ($gp130^{-/-}$) mice 30 min after i.v. stimulation with NaCl, leptin, or recombinant CNTF. (*d*) Quantification of p-STAT3-positive POMC cells after CNTF stimulation in control (CO) and $gp130^{\Delta POMC}$ (KO) mice (mean ± SEM of three animals in each group) ($P < 0.001$). (*e*) Quantitative and spatial analysis of POMC neurons in control (open bars) and $gp130^{\Delta POMC}$ (filled bars) mice ($n = 3$ of each genotype).

receptors such as the CNTF receptor, without abolishing gp130-independent cytokine receptor signaling such as that mediated by the leptin receptor.

Unaltered POMC Neuron Number and Stress Response in $gp130^{\Delta POMC}$ Mice. gp130 has been demonstrated to play a critical role in neurogenesis (16). Thus, we next determined whether lack of functional gp130 signaling alters the number or distribution of hypothalamic POMC neurons. This analysis revealed equal numbers and distribution of POMC neurons in both control and $gp130^{\Delta POMC}$ mice (Fig. 1*e*). These data indicate that disrupted gp130 signaling in our animals did not affect neurogenesis and cell survival of POMC neurons.

Consistent with the expression pattern of endogenously expressed POMC, the only non-hypothalamic site of recombination detectable in *PomcCre*-transgenic mice was the pituitary (Fig. 2*a*). Because cytokines that signal through gp130-dependent receptors such as leukemia inhibiting factor (LIF) and IL-6 have been demonstrated to regulate adrenocorticotropin expression and release in cultured pituitary cells (17), we next characterized the functional stress response of $gp130^{\Delta POMC}$ mice. *Pomc* mRNA expression in the pituitary of control and $gp130^{\Delta POMC}$ mice did not show a significant difference (Fig. 2*b*). To directly determine the stress response in control and $gp130^{\Delta POMC}$ mice, we used two paradigms activating the corticotropic response via distinct mechanisms, i.e., restraint stress and LPS injection. Both stimuli dramatically increased plasma corticosterone concentrations to a comparable extent in control and $gp130^{\Delta POMC}$ mice (Fig. 2*c*). As expected, LPS injection resulted in a profound increase of circulating IL-6 concentrations (18) (Fig. 2*d*). This increase was indistinguishable between control and $gp130^{\Delta POMC}$ mice (Fig. 2*d*). Taken together, these data indicate that inactivation of gp130 signaling in POMC cells of the hypothalamus and pituitary does not impair responses to restraint and LPS-induced stress in these animals.

Normal Energy and Glucose Homeostasis in $gp130^{\Delta POMC}$ Mice. To determine the importance of endogenous gp130-dependent signaling in POMC cells on the regulation of energy homeostasis, we first

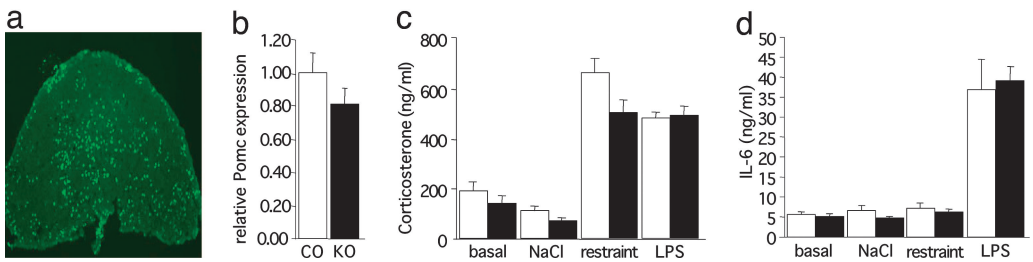

Fig. 2. Unaltered stress response in $gp130^{\Delta POMC}$ mice. (*a*) Immunohistochemistry for enhanced GFP performed in the pituitary of *PomcCre*, *Z/EG* mice. (*b*) Relative expression of *Pomc* mRNA in pituitaries of control (CO) and $gp130^{\Delta POMC}$ (KO) mice ($n = 7$–8). (*c*) Plasma corticosterone concentrations: basal and 1 h after NaCl injection, restraint stress, or LPS treatment in control (open bars; $n = 6$–10) and $gp130^{\Delta POMC}$ (filled bars; $n = 7$–12) mice. (*d*) IL-6 plasma concentrations: basal and 1 h after NaCl injection, restraint stress, or LPS treatment in control (open bars; $n = 6$) and $gp130^{\Delta POMC}$ (filled bars; $n = 7$) mice.

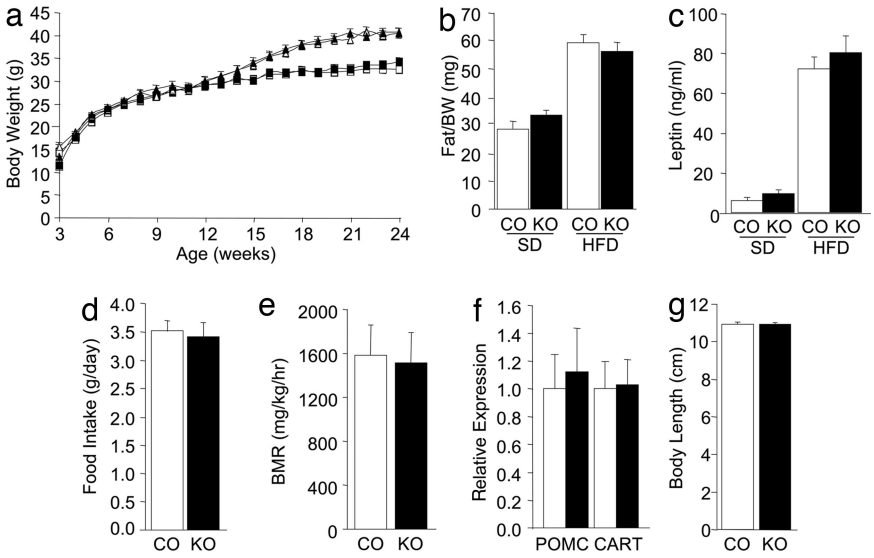

Fig. 3. Unaltered energy homeostasis in *gp130*$^{\Delta POMC}$ mice. (*a*) Body-weight curve of control (open squares and open triangles) and *gp130*$^{\Delta POMC}$ (filled squares and filled triangles) mice on standard diet (SD) (squares; $n = 12–18$) and high-fat diet (HFD) (triangles; $n = 12–31$). (*b*) Epigonadal fat pads were dissected and weighed. Data represent the mean ± SEM of 14–31 mice in each group. (*c*) Serum leptin levels of control ($n = 10–16$) and *gp130*$^{\Delta POMC}$ ($n = 10–16$) mice on SD and HFD at the age of 24 weeks. (*d*) Daily food intake of control ($n = 6$) and *gp130*$^{\Delta POMC}$ ($n = 9$) mice at the age of 11 weeks. (*e*) Basal metabolic rate (BMR) of control (CO) ($n = 6$) and *gp130*$^{\Delta POMC}$ (KO) ($n = 9$) mice at the age of 11 weeks. (*f*) Relative expression of POMC and CART in control (open bars; $n = 7–8$) and *gp130*$^{\Delta POMC}$ (filled bars; $n = 6–7$) mice. (*g*) Body length of control ($n = 13$) and *gp130*$^{\Delta POMC}$ ($n = 13$) mice.

monitored the body weight of control and *gp130*$^{\Delta POMC}$ mice from weaning until 6 months of age. This analysis revealed no change in body weight in the presence of POMC-restricted gp130 deficiency both under standard and high-fat diets (Fig. 3*a*). White adipose tissue mass and circulating plasma leptin concentrations were indistinguishable between control and *gp130*$^{\Delta POMC}$ mice (Fig. 3 *b* and *c*). In control and *gp130*$^{\Delta POMC}$ mice, there was an increase in adipose tissue mass and plasma leptin concentrations upon exposure to high-fat diet (Fig. 3 *b* and *c*). Food intake and basal metabolic rate were also indistinguishable between control and *gp130*$^{\Delta POMC}$ mice (Fig. 3 *d* and *e*). The expression of anorexigenic neuropeptides such as POMC and cocaine- and amphetamine-related transcript (CART) was unaltered in control and *gp130*$^{\Delta POMC}$ mice (Fig. 3*f*). Body length was indistinguishable between control and *gp130*$^{\Delta POMC}$ mice, a further indication of intact function of the melanocortin pathway in the absence of gp130 signaling in POMC neurons (Fig. 3*g*).

Consistent with unaltered energy homeostasis in *gp130*$^{\Delta POMC}$ mice, these animals exhibited normal glucose metabolism as assessed by glucose tolerance tests, insulin tolerance tests, and blood glucose and plasma insulin concentrations (Fig. 5 *a*, *c*, *e*, and *f*, which is published as supporting information on the PNAS web site). Exposure to high-fat diet resulted in impaired glucose tolerance, increased blood glucose concentrations, and elevated plasma insulin concentrations as an indirect measure of insulin resistance in a similar manner in control and *gp130*$^{\Delta POMC}$ mice (Fig. 5 *b* and *d–f*). Taken together, these data indicate that gp130 signaling in POMC neurons is dispensable for normal control of body weight, food intake, energy expenditure, and glucose metabolism.

Blunted Anorectic Response to Intracerebroventricularly (i.c.v.) Injected CNTF in *gp130*$^{\Delta POMC}$ Mice. To analyze the effect of exogenous CNTF on food intake, we implanted cannulae into the lateral ventricle of female and male control and *gp130*$^{\Delta POMC}$ mice. In females, analysis of food intake 4 h after CNTF injection revealed a reduction in food intake in control mice by ≈80% compared with 0.9% NaCl injection (Fig. 4*a*). Strikingly, however, this effect was severely blunted in *gp130*$^{\Delta POMC}$ mice, which exhibited only a 35% reduction in food intake (Fig. 4*a*). Similarly, in females, food intake over 24 h after a single injection of CNTF was significantly reduced by 40% in control animals but only resulted in a decrease of 18% in *gp130*$^{\Delta POMC}$ mice (Fig. 4*a*). In addition, CNTF reduced body weight significantly 24 h after injection in control females but exhibited only a minor effect in *gp130*$^{\Delta POMC}$ mice (Fig. 4*b*). Similar results were obtained when male control and *gp130*$^{\Delta POMC}$ mice were acutely treated with CNTF: 6-h food intake after single injection was significantly reduced by 60% in control animals, whereas *gp130*$^{\Delta POMC}$ mice failed to exhibit a significant reduction of food intake (Fig. 4*c*). Body weight significantly decreased by 4% in CNTF-treated controls, whereas it remained unchanged in *gp130*$^{\Delta POMC}$ mice (Fig. 4*d*). Taken together, CNTF very rapidly and severely impairs food intake over a 24-h period in control animals, an effect that is blunted in *gp130*$^{\Delta POMC}$ mice.

CNTF Fails to Induce c-Fos Immunoreactivity in the Paraventricular Nucleus (PVN) of *gp130*$^{\Delta POMC}$ Mice. The PVN of the hypothalamus is a major site of action of POMC efferents in the regulation of feeding (19). Therefore, we analyzed the activation of PVN neurons in response to acute CNTF treatment in control and *gp130*$^{\Delta POMC}$ mice. In control animals, CNTF evoked a strong induction of c-Fos immunoreactivity in the PVN (Fig. 4 *e* and *f*). Strikingly, however, CNTF treatment completely failed to enhance c-Fos immunoreactivity in the PVN of male *gp130*$^{\Delta POMC}$ mice (Fig. 4 *e* and *f*). Thus, CNTF application acutely and strongly activates neurons in the PVN that are characterized as important mediators of energy homeostasis regulation (19). The absence of PVN neuronal activation in response to CNTF application in *gp130*$^{\Delta POMC}$ mice clearly indicates that PVN activation critically depends on functional CNTF signaling in POMC neurons.

Discussion

CNTF has provided an attractive therapeutic tool for the treatment of obesity, although its clinical use has been limited due to the development of neutralizing antibodies in patients treated with a recombinant variant of CNTF (20). Despite intense research over the years, the exact site of CNTF action in mediating its anorectic effect has not been resolved.

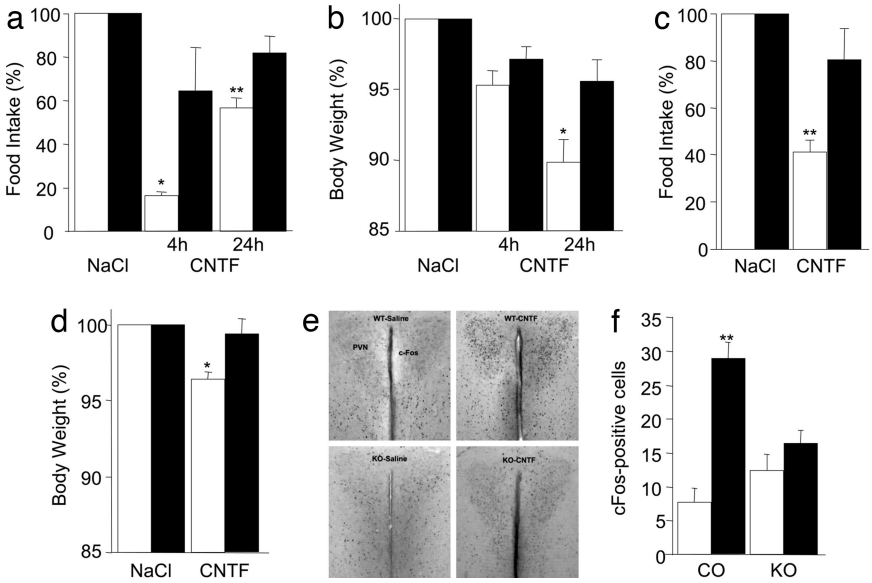

Fig. 4. *gp130*$^{\Delta POMC}$ mice are resistant to the acute anorectic effect of i.c.v. injected CNTF. i.c.v. injection of either 0.9% NaCl or 1 μg of recombinant rat CNTF into the lateral ventricle of 13- to 15-week-old mice. (*a*) Food intake of female control (open bars) and *gp130*$^{\Delta POMC}$ (filled bars) mice, 0.9% NaCl-treated, 4 and 24 h after i.c.v. CNTF injection (mean ± SEM of 9–10 animals in each group) ($P < 0.05$, $P < 0.01$). (*b*) Body weight of female control (open bars) and *gp130*$^{\Delta POMC}$ (filled bars) mice, 0.9% NaCl-treated, 4 and 24 h after CNTF injection (mean ± SEM of 9–10 animals in each group) ($P < 0.05$). (*c*) Food intake of male control (open bars) and *gp130*$^{\Delta POMC}$ (filled bars) mice, 0.9% NaCl-treated, 6 h after i.c.v. CNTF injection (mean ± SEM of 6–16 animals in each group) ($P < 0.01$). (*d*) Body weight of male control (open bars) and *gp130*$^{\Delta POMC}$ (filled bars) mice, 0.9% NaCl-treated, 6 h after i.c.v. CNTF injection (mean ± SEM of 6–16 animals in each group) ($P < 0.05$). (*e*) c-Fos expression in the PVN of control and *gp130*$^{\Delta POMC}$ mice 6 h after i.c.v. injection of 0.9% NaCl or CNTF. (*f*) Quantification of c-Fos-positive cells in the PVN of control and *gp130*$^{\Delta POMC}$ mice 6 h after i.c.v. injection of 0.9% NaCl or CNTF.

Here, we show that the POMC-specific deletion of gp130 (*gp130*$^{\Delta POMC}$) has no impact on body weight, food intake, energy expenditure, and glucose metabolism, indicating that endogenous CNTF does not influence energy homeostasis via POMC neurons. In contrast, pharmacological doses of CNTF, injected i.c.v., resulted in a blunted anorectic response in *gp130*$^{\Delta POMC}$ mice, associated with abolished neuronal activation in the PVN. Thus, our current experiments define a functional neural circuit in which CNTF signaling in POMC neurons is essential for CNTF's acute inhibitory effect on food intake and the activation of PVN neurons. These results are in line with the fact that CNTF engages similar intracellular signaling mechanisms to those activated by leptin stimulation (7, 11).

Nevertheless, the pattern of STAT3 phosphorylation within the hypothalamus was different after stimulation with CNTF vs. leptin. This is consistent with previous studies reporting a robust phospho (p)-STAT3 staining in the ventromedial part of the ARC after CNTF stimulation, whereas leptin-stimulated STAT3 phosphorylation was more prominent in the lateral ARC and the ventromedial hypothalamus (6). However, even though this points to a differential expression of CNTF and leptin receptors within different neuronal populations of the ARC, our functional results reveal that CNTF signaling plays a critical role in POMC cells. Thus, CNTF and leptin seem to target at least this cell type similarly.

Our data reveal a blunted reduction of body weight and food intake in *gp130*$^{\Delta POMC}$ females upon acute CNTF treatment. However, in male *gp130*$^{\Delta POMC}$ mice, POMC-specific deletion of gp130 completely abolished the anorectic response to i.c.v. applied CNTF. Even though the underlying mechanism for this sexually dimorphic phenotype remains unsolved, our data are in line with other studies using genetic mouse models of obesity (21–23) or analyzing the effect of centrally administered agents such as insulin and leptin on energy homeostasis (24) also finding different phenotypes and pharmacological responses depending on gender.

In this study, we have addressed the acute pharmacological effect of centrally administered CNTF, but analyzing the effect of chronic CNTF treatment in *gp130*$^{\Delta POMC}$ mice will certainly provide additional important information. CNTF exhibits a unique feature, which is protection from weight rebound upon termination of treatment (7). Therefore, it will be crucial to determine whether this long-term protection also depends on functional gp130 signaling in POMC neurons.

More recently, additional intriguing mechanisms for CNTF action have been described. CNTF has been demonstrated to induce neurogenesis in the ARC of the adult brain. Importantly, this effect appeared to be necessary for protection against weight rebound (25). Kokoeva *et al.* also provided evidence that newly proliferated neurons exhibit both neuropeptide Y and POMC expression. Therefore, one could speculate that CNTF's effect on neurogenesis requires gp130 signaling in adult neuronal stem cells before the acquirement of a POMC phenotype. According to this model, the protective effect against weight rebound would be retained in *gp130*$^{\Delta POMC}$ mice.

Furthermore, it has become evident that CNTF also exerts effects in peripheral tissues such as skeletal muscle and liver to improve metabolism via activation of AMP-dependent kinases (AMPK) (26, 27). Therefore, *gp130*$^{\Delta POMC}$ mice as well as mice with targeted disruption of gp130 signaling in peripheral organs will allow for the definition of the contribution of organ-specific gp130 signaling to the improvement of glucose metabolism and sustained weight loss upon chronic CNTF treatment.

Moreover, *gp130*$^{\Delta POMC}$ mice provide an excellent tool to dissect the primary site of other cytokines acting in the central nervous system to regulate energy homeostasis and signaling via gp130-dependent receptor complexes. These comprise IL-6 and the leukemia inhibitory factor (LIF) (28). Therefore, it will be interesting to analyze the effect of centrally administered IL-6 and LIF in *gp130*$^{\Delta POMC}$ mice and in mice with targeted disruption of gp130 in other neuronal populations such as AgRP/neuropeptide Y neurons. Ultimately, these experiments will allow for the dissection of neuronal networks targeted by different cytokines to regulate energy homeostasis and metabolism.

Methods

Animals. All animal procedures were conducted in compliance with protocols approved by local government authorities (Bezirksregierung Köln) and were in accordance with National Institutes of Health guidelines. Mice were housed in groups of three to five at 22–24°C in a 12-h light/12-h dark cycle with lights on at 6 a.m. Animals were fed either regular chow food (Global Rodent T.2018.R12 from Harlan Teklad, containing 12% of calories from fat) or a high-fat diet (C1057 from Altromin, containing 55.2% of calories from fat). Water was available ad libitum, and food was only withdrawn if required for an experiment. Body weight was measured once per week. At the end of the study period, the animals were killed under isoflurane anesthesia.

Generation of *PomcCre-gp130$^{lox/lox}$* Mice. *PomcCre* mice (14) were mated with *gp130$^{lox/lox}$* mice (13), and a breeding colony was maintained by mating *gp130$^{lox/lox}$* with *PomcCre-gp130$^{lox/lox}$* mice. *gp130^{lox}* mice had been backcrossed for at least five generations on a C57BL/6 background, and *PomcCre* mice (initially established on an FVB background) had been backcrossed for two generations on a C57BL/6 background before intercrossing them with *gp130^{lox}* mice. Only animals from the same mixed background strain generation were compared with each other. *PomcCre* mice were genotyped by PCR as described in ref. 14. *gp130* mice were genotyped by PCR with the following primers: 5gp130, 5′-GGT GGC TGA TTC ACC TGC A-3′; and 3gp130, 5′-TAC GCT GGG CAG CGT CCT-3′. For visualization of Cre-mediated recombination, mice were crossed with either the indicator strain *Rosa*(*lacZ reporter*) (Fig. 6, which is published as supporting information on the PNAS web site) (29) or the *Z/EG* reporter strain (15).

Restraint Stress and LPS Treatment. Mice were adapted to gentle handling for ≈8 weeks before the experiment. To determine basal serum corticosterone and IL-6 levels, blood was drawn from the tail vein during the first 3 h of the light phase. The next day, mice were subjected to 1 h of restraint stress at the same time of the light phase. Restraint stress was achieved by enclosing the animals in a plastic tube with a diameter of 3 cm and openings at both ends for tail and nose. At the end of the experiment, blood samples were again drawn from the tail vein.

Seven days later, the animals were injected i.p. with 0.9% NaCl during the first 3 h of the light phase, and blood was collected from the tail vein 1 h after injection. After 5 days of recovery, each mouse received an i.p. injection of 300 μg of LPS (L2630 from Sigma) 1 h after injection blood samples were taken. Two days after LPS injection, the animals were killed under isoflurane anesthesia.

Glucose and Insulin Tolerance Tests. Glucose and insulin tolerance tests were performed as described in ref. 30.

Indirect Calorimetry and Food Intake. All measurements were performed with the Comprehensive Laboratory Animal Monitoring System (CLAMS) (OXYMAX; Columbus Instruments, Columbus, OH). Mice were placed at room temperature (22–24°C) in 3.0-liter chambers of the CLAMS open circuit calorimetry. Settling time was set at 150 s, and measuring time was set at 60 s with room air as reference. Food and water were provided ad libitum in the appropriate devices. Mice were allowed to acclimatize in the chambers for 24 h. Parameters of indirect calorimetry were measured for at least the following 72 h. Food intake was measured continuously in the CLAMS during the experiment. The data presented are average values obtained in these recordings.

Western Blot Analysis. Indicated tissues were dissected and homogenized in homogenization buffer with a Polytron homogenizer (IKA Werke, Staufen, Germany), and Western blot analyses were performed as described in ref. 31 with antibodies raised against gp130 (sc-656 from Santa Cruz Biotechnology) and Pten (MS-1250-P from NeoMarkers) as loading control.

Hypothalamic Neuropeptide Expression. Measurements of mRNA levels were carried out by quantitative RT-PCR on RNA extracted from dissected hypothalamic or pituitary tissue. Total RNA for each hypothalamus was quantified by spectrophotometry after purification with the Qiagen RNeasy kit. Two hundred nanograms of each total RNA sample was reverse-transcribed and PCR-amplified by using the TaqMan-principles ABI PRISM 7700 sequence detection system (Applied Biosystems). Efficiency for the primers was estimated from standard curves made with serial cDNA dilutions.

Analytical Procedures. Blood glucose levels and insulin and leptin serum levels were determined as described in ref. 30. IL-6 serum levels were measured by ELISA with mouse standards according to the manufacturer's guidelines (BD OptEIA mouse IL-6 ELISA kit; BD Biosciences Pharmingen). Corticosterone serum levels were determined by RIA using mouse standards according to the manufacturer's guidelines (ImmuChem Double Antibody Corticosterone ^{125}I RIA kit; ICN).

Statistical Methods. Data were analyzed for statistical significance by using a two-tailed unpaired Student *t* test.

i.c.v. Cannula Implantation. Twelve-week-old mice were anesthetized by i.p. injection of Avertin (240 mg/kg) (2,2,2-tribromoethanol; Sigma) and placed in a stereotactic device. A sterile osmotic pump connector cannula (Bilaney Consultants, Düsseldorf, Germany) was implanted into the lateral brain ventricle (0.2 mm posterior and 1.0 mm lateral relative to bregma and 2.3 mm below the surface of the skull). The support plate of the catheter was attached to the skull with superglue. The catheter was prefilled with 0.9% NaCl and connected to a sealed microrenathane catheter (MRE-025 from Braintree Scientific, Braintree, MA).

i.c.v. Injection. After 7 days of recovery, 2 μl of recombinant rat CNTF (0.5 mg/ml; 557-NT/CF from R & D Systems) or 0.9% NaCl was injected, and 1 μl of 0.9% NaCl was postinjected to ensure a complete drug administration to the brain. To avoid a backflow, the catheter was sealed. Injections were performed under isoflurane anesthesia 1 h before the onset of the dark cycle.

Food intake and body weight were measured 4 and 24 h after the injection for females and 6 h after the injection for males. The correct position of the i.c.v. cannula was verified by injection of methyl blue after the mice were killed.

Tissue Preparation for Immunocytochemistry and Immunocytochemical Procedures. Control and *gp130$^{\Delta POMC}$* mice were mated with *RosaArte26* reporter mice (29). At the age of 10 weeks, mice fed ad libitum received one i.v. injection of 5 μg of recombinant rat CNTF, 20 μg of leptin (L3772 from Sigma), or 0.9% NaCl into the tail vein. Thirty minutes after injection, the mice were perfused with 0.9% NaCl followed by 4% paraformaldehyde, and the brains were extracted, kept in 4% paraformaldehyde overnight at 4°C, and stored in 20% sucrose at 4°C.

For one series, we performed double-labeling of p-STAT3 and β-galactosidase (indicating POMC-expressing neurons) using free-floating immunohistochemistry as described in ref. 32. In brief, sections were washed, pretreated with 100% methanol/0.3% glycine/0.03% SDS, and blocked in 3% normal donkey serum followed by incubation of the primary antibodies [rabbit anti-p-STAT3 (1:3,000 dilution; Cell Signaling Technology, Beverly, MA) and goat anti-β-galactosidase (1:3,000 dilution; Biogenesis, Poole, U.K.)] for 48 h at 4°C. Secondary labeling was done with anti-rabbit Alexa 488 (Invitrogen/Molecular Probes) and biotinylated anti-

goat antibody (1:200; Jackson ImmunoResearch) followed by streptavidin-Alexa 568 (1:200) for detection of p-STAT3 and β-galactosidase antibodies. Sections were mounted onto gelatin-coated slides, dried, and coverslipped by using mounting media (ProLong Gold; Invitrogen/Molecular Probes). Fluorescence signals were detected under a fluorescent microscope (BX51; Olympus), and representative pictures of the ARC were taken with a digital color camera (DP70; Olympus).

Fot better visualization of GFP expression after Cre-recombination, brain sections (25 μm) of double-heterozygous *PomcCre Z/EG* mice were washed, pretreated with 0.3% H_2O_2, blocked with PBT-Azide containing 3% donkey serum, and incubated overnight with primary antibody (anti-GFP rabbit serum, 1:10,000; A6455 from Invitrogen/Molecular Probes). Incubation with secondary antibody (anti-rabbit IgG, 1:500; 711-065-125 from Jackson ImmunoResearch) was followed by incubation with the VECTASTAIN Elite ABC kit (Vector Laboratories) for 1 h and 0.4% DAB/0.01% H_2O_2. Afterward the sections were mounted onto gelatin-coated slides and covered with glycerin.

Pituitary was stained with the same antibodies, using the Tyramide Signal Amplification kit (TSA Plus Fluorescence Systems; PerkinElmer).

POMC Cell Counting. Quantification of β-galactosidase-positive POMC cells was done as described in ref. 32. In brief, every fourth section throughout the ARC was taken and allocated rostral to caudal to visualize the distribution of POMC neurons throughout the ARC. By using Adobe PHOTOSHOP software, β-galactosidase-positive neurons were counted and marked digitally to prevent multiple counts. Cell counts were performed on three animals per group. The percentage of double-positive cells compared with the total amount of β-galactosidase-positive POMC cells after CNTF stimulation was also determined by cell counting.

Immunostaining for c-Fos and Quantification. As described above, catheter-implanted animals received an injection of either 0.9% NaCl or CNTF 1 h before onset of the dark phase. Six hours later, the mice were anesthetized by using Avertin and perfused with 0.9% NaCl followed by Somogyi–Takagi fixative. The brains were dissected, kept in glutaraldehyde-free fixative at 4°C for at least 2 h, and stored in 0.1 M phosphate buffer at 4°C until further preparation.

Free-floating brain sections (50 μm) containing the PVN were immunostained for c-Fos [rabbit α-c-Fos, Oncogene (EMD Bioscience) used at 1:20,000] by our standard protocol using diaminobenzidine as the chromagen as described in ref. 33. Sections were examined under a Zeiss Axioplan 2 microscope outfitted with an AxioCam HRc camera and AXIOVISION 4.2 imaging software. Every section containing the PVN ($n = 4$) was examined for each animal (with the operator blinded to the experimental conditions). For each hemisphere of the PVN, at a magnification of ×40, a single plane of focus was chosen and a black and white image was captured; a 100-μm^2 box was placed in the center of the PVN. All of the c-Fos-labeled cell nuclei were counted within the box for each section. Only those labeled nuclei that were clearly in the plane of focus were selected. The results were expressed as the number of c-Fos-labeled cells per 100-μm^2 area of the PVN.

We thank Gisela Schmall for secretarial assistance; F. Schwenk and J. Seibler (Artemis Pharmaceuticals) for providing *Rosa26(LacZ reporter)* mice; and N. Balthasar, R. Coppari, J. Elmquist, and B. B. Lowell for generously providing the POMC-Cre mice. This work was supported by Zentrum für Molekulare Medizin der Universität zu Köln Grant TV2 (to J.C.B.), European Union Grant LSHM-CT-2003-503041 (to J.C.B.), a grant from the Köln Fortune Program (to L.P.), a grant from the Fritz Thyssen Stiftung (to J.C.B.), American Heart Association Grant AHA 0535298N (to H.M.), and National Institutes of Health Grants DK-01445 and DK-060711 (to T.L.H.).

1. Munzberg, H. & Myers, M. G., Jr. (2005) *Nat. Neurosci.* **8,** 566–570.
2. Zabeau, L., Defeau, D., Van der Heyden, J., Iserentant, H., Vandekerckhove, J. & Tavernier, J. (2004) *Mol. Endocrinol.* **18,** 150–161.
3. Banks, W. A. & Farrell, C. L. (2003) *Am. J. Physiol.* **285,** E10–E15.
4. Munzberg, H., Flier, J. S. & Bjorbaek, C. (2004) *Endocrinology* **145,** 4880–4889.
5. MacLennan, A. J., Vinson, E. N., Marks, L., McLaurin, D. L., Pfeifer, M. & Lee, N. (1996) *J. Neurosci.* **16,** 621–630.
6. Anderson, K. D., Lambert, P. D., Corcoran, T. L., Murray, J. D., Thabet, K. E., Yancopoulos, G. D. & Wiegand, S. J. (2003) *J. Neuroendocrinol.* **15,** 649–660.
7. Lambert, P. D., Anderson, K. D., Sleeman, M. W., Wong, V., Tan, J., Hijarunguru, A., Corcoran, T. L., Murray, J. D., Thabet, K. E., Yancopoulos, G. D. & Wiegand, S. J. (2001) *Proc. Natl. Acad. Sci. USA* **98,** 4652–4657.
8. Pu, S., Dhillon, H., Moldawer, L. L., Kalra, P. S. & Kalra, S. P. (2000) *J. Neuroendocrinol.* **12,** 827–832.
9. Kalra, S. P., Xu, B., Dube, M. G., Moldawer, L. L., Martin, D. & Kalra, P. S. (1998) *Neurosci. Lett.* **240,** 45–49.
10. Prima, V., Tennant, M., Gorbatyuk, O. S., Muzyczka, N., Scarpace, P. J. & Zolotukhin, S. (2004) *Endocrinology* **145,** 2035–2045.
11. Kelly, J. F., Elias, C. F., Lee, C. E., Ahima, R. S., Seeley, R. J., Bjorbaek, C., Oka, T., Saper, C. B., Flier, J. S. & Elmquist, J. K. (2004) *Diabetes* **53,** 911–920.
12. Gropp, E., Shanabrough, M., Borok, E., Xu, A. W., Janoschek, R., Buch, T., Plum, L., Balthasar, N., Hampel, B., Waisman, A., *et al.* (2005) *Nat. Neurosci.* **8,** 1289–1291.
13. Betz, U. A., Bloch, W., van den Broek, M., Yoshida, K., Taga, T., Kishimoto, T., Addicks, K., Rajewsky, K. & Muller, W. (1998) *J. Exp. Med.* **188,** 1955–1965.
14. Balthasar, N., Coppari, R., McMinn, J., Liu, S. M., Lee, C. E., Tang, V., Kenny, C. D., McGovern, R. A., Chua, S. C., Jr., Elmquist, J. K. & Lowell, B. B. (2004) *Neuron* **42,** 983–991.
15. Novak, A., Guo, C., Yang, W., Nagy, A. & Lobe, C. G. (2000) *Genesis* **28,** 147–155.
16. Barnabe-Heider, F., Wasylnka, J. A., Fernandes, K. J., Porsche, C., Sendtner, M., Kaplan, D. R. & Miller, F. D. (2005) *Neuron* **48,** 253–265.
17. Perez Castro, C., Carbia Nagashima, A., Paez Pereda, M., Goldberg, V., Chervin, A., Carrizo, G., Molina, H., Renner, U., Stalla, G. K. & Arzt, E. (2001) *J. Endocrinol.* **169,** 539–547.
18. Kariagina, A., Romanenko, D., Ren, S. G. & Chesnokova, V. (2004) *Endocrinology* **145,** 104–112.
19. Balthasar, N., Dalgaard, L. T., Lee, C. E., Yu, J., Funahashi, H., Williams, T., Ferreira, M., Tang, V., McGovern, R. A., Kenny, C. D., *et al.* (2005) *Cell* **123,** 493–505.
20. Ettinger, M. P., Littlejohn, T. W., Schwartz, S. L., Weiss, S. R., McIlwain, H. H., Heymsfield, S. B., Bray, G. A., Roberts, W. G., Heyman, E. R., Stambler, N., *et al.* (2003) *J. Am. Med. Assoc.* **289,** 1826–1832.
21. Lewitt, M. S. & Brismar, K. (2002) *Int. J. Obes. Relat. Metab. Disorders* **26,** 1296–1300.
22. Costet, P., Legendre, C., More, J., Edgar, A., Galtier, P. & Pineau, T. (1998) *J. Biol. Chem.* **273,** 29577–29585.
23. Bruning, J. C., Gautam, D., Burks, D. J., Gillette, J., Schubert, M., Orban, P. C., Klein, R., Krone, W., Muller-Wieland, D. & Kahn, C. R. (2000) *Science* **289,** 2122–2125.
24. Woods, S. C., Gotoh, K. & Clegg, D. J. (2003) *Exp. Biol. Med. (Maywood, N.J.)* **228,** 1175–1180.
25. Kokoeva, M. V., Yin, H. & Flier, J. S. (2005) *Science* **310,** 679–683.
26. Watt, M. J., Dzamko, N., Thomas, W. G., Rose-John, S., Ernst, M., Carling, D., Kemp, B. E., Febbraio, M. A. & Steinberg, G. R. (2006) *Nat. Med.* **12,** 541–548.
27. Watt, M. J., Hevener, A., Lancaster, G. I. & Febbraio, M. A. (2006) *Endocrinology* **147,** 2077–2085.
28. Wallenius, V., Wallenius, K., Ahren, B., Rudling, M., Carlsten, H., Dickson, S. L., Ohlsson, C. & Jansson, J. O. (2002) *Nat. Med.* **8,** 75–79.
29. Seibler, J., Zevnik, B., Kuter-Luks, B., Andreas, S., Kern, H., Hennek, T., Rode, A., Heimann, C., Faust, N., Kauselmann, G., *et al.* (2003) *Nucleic Acids Res.* **31,** e12.
30. Rohl, M., Pasparakis, M., Baudler, S., Baumgartl, J., Gautam, D., Huth, M., De Lorenzi, R., Krone, W., Rajewsky, K. & Bruning, J. C. (2004) *J. Clin. Invest.* **113,** 474–481.
31. Schubert, M., Gautam, D., Surjo, D., Ueki, K., Baudler, S., Schubert, D., Kondo, T., Alber, J., Galldiks, N., Kustermann, E., *et al.* (2004) *Proc. Natl. Acad. Sci. USA* **101,** 3100–3105.
32. Munzberg, H., Huo, L., Nillni, E. A., Hollenberg, A. N. & Bjorbaek, C. (2003) *Endocrinology* **144,** 2121–2131.
33. Palkovits, M., Baffi, J. S., Berzsenyi, P. & Horvath, E. J. (1997) *Eur. J. Pharmacol.* **331,** 53–63.